Entropy production in quantum Yang–Mills mechanics in the semiclassical approximation

Hidekazu Tsukiji[1],*, Hideaki Iida[2], Teiji Kunihiro[2], Akira Ohnishi[1], and
Toru T. Takahashi[3]

[1]*Yukawa Institute for Theoretical Physics, Kyoto University, Kyoto 606-8502, Japan*
[2]*Department of Physics, Faculty of Science, Kyoto University, Kyoto 606-8502, Japan*
[3]*Gunma National College of Technology, Gunma 371-8530, Japan*
*E-mail: tsukiji@yukawa.kyoto-u.ac.jp

. . . .

We discuss thermalization of isolated quantum systems by using the Husimi–Wehrl entropy evaluated in the semiclassical treatment. The Husimi–Wehrl entropy is the Wehrl entropy obtained by using the Husimi function for the phase space distribution. The time evolution of the Husimi function is given by smearing the Wigner function, whose time evolution is obtained in the semiclassical approximation. We show the efficiency and usefulness of this semiclassical treatment in describing the entropy production of a couple of quantum-mechanical systems, whose classical counter-systems are known to be chaotic. We propose two methods to evaluate the time evolution of the Husimi–Wehrl entropy, the test-particle method and the two-step Monte Carlo method. We demonstrate the characteristics of the two methods by numerical calculations, and show that simultaneous application of the two methods ensures the reliability of the results of the Husimi–Wehrl entropy at a given time.

. . . .

Subject Index   A52, A56, D31

1. Introduction

The thermalization process or entropy creation of isolated quantum systems is a long-standing issue, but not a well understood problem. Relevant systems include the early universe, where the transition from a vacuum state to a thermalized state occurs at the end of cosmic inflation, and the quantum chromodynamics (QCD) matter created in the initial stage of relativistic heavy-ion collisions, where thermal matter should be formed in a rather short time. It is known that both systems are well described in the semiclassical approximation, and, moreover, a chaotic behavior of the classical limit may play some role in the entropy production. The present paper is concerned with the entropy production of an isolated quantum system for which the semiclassical approximation is valid and the classical counterpart may show a chaotic behavior.

To describe entropy in a pure quantum system, one may, of course, adopt the von Neumann entropy [1,2] as quantum-mechanical entropy given by

$$S_{vN} = -\mathrm{Tr}\left[\rho \log \rho\right], \tag{1}$$

where ρ is the density matrix. For a pure state, however, ρ is idempotent, $\rho^2 = \rho$, implying that the eigenvalue of ρ is 0 or 1, and the von Neumann entropy is zero. Even if we start from a mixed state, the time evolution described by a unitary operator will never lead to entropy growth. On the other hand, the entropy production in a rarefied gas composed of classical or quantum-mechanical particles

can be well described by an analog of Boltzmann's H function given in terms of the distribution function $f(q, p)$:

$$S = -\int \frac{d^D q\, d^D p}{(2\pi\hbar)^D} f(q, p) \log f(q, p). \tag{2}$$

It is noteworthy that a phase space description is desirable for making the classical–quantum correspondence clear, and is even natural when the semiclassical approximation is valid. The standard method for such a description is to use the celebrated Wigner function [3], which is defined as a Wigner transform of the density matrix: The Wigner function $f_W(q, p)$ can be regarded as a quasi phase space distribution function. The use of the Wigner function as the phase space distribution function ($f(q, p) = f_W(q, p)$ in Eq. (2)), however, has essential drawbacks: First, the Wigner function is, actually, not a genuine distribution function; f_W can be negative, which prevents us from calculating the entropy density according to Eq. (2). Second, the entropy defined by Eq. (2) given in terms of the Wigner function f_W does not grow in time, because the Wigner transform only gives an equivalent description of the quantum system in terms of, say, the q- or p-representation [4–8]. Some coarse graining of the phase space is needed to describe the entropy production.

In a classical chaotic system, two adjacent points in the phase space depart from each other exponentially in time. If the available phase space volume is limited, the exponentially diffusing classical trajectories have to be folded in a complicated manner in the phase space. After a certain time starting from a localized phase space cell, a given phase space cell $(2\pi\hbar)^D$ consists of the mixture of trajectories stemming from the initially occupied localized cell and vacant regions not yet visited. Since we cannot distinguish the phase space points in a cell due to the uncertainty principle, it is reasonable to define a phase space distribution as a smeared or coarse-grained function over the phase space cell.

We adopt the Husimi function $f_H(q, p)$ [9] as such a coarse-grained distribution function, which is defined as the expectation value of the density matrix with respect to a coherent state $|z\rangle$. It is readily shown that $f_H(q, p)$ is *semi-positive definite*, $f_H \geq 0$, and a coarse-grained function of the Wigner function, as will be shown in a later section. It is shown [10,11] that the Husimi function faithfully describes the characteristic properties of the underlying classical system, and has been utilized to identify the chaotic remnants in quantum systems [10–13]. Thus a natural candidate of the quantum-mechanical entropy is given by (2) with $f(q, p)$ being substituted by the Husimi function $f_H(q, p)$. This entropy was introduced by Wehrl [14] and may be called the Wehrl entropy, although he himself called it classical entropy and failed to identify the distribution function $f_H(q, p)$ with the Husimi function: such an identification was made later [15]. We refer to the Wehrl entropy obtained by using the Husimi function as the *Husimi–Wehrl (HW) entropy* [16]:

$$S_{HW} = -\int \frac{d^D q\, d^D p}{(2\pi\hbar)^D} f_H(q, p) \log f_H(q, p). \tag{3}$$

It is worth mentioning that the HW entropy can be a good measure for the quantum entanglement of a system including quantum optical systems [17,18]. For the 1D case, there is a minimum of $S_{HW} = 1$ [19,20], in contrast to the von Neumann entropy, which takes $S_{vN} = 0$ in the ground state. It is also shown that the HW entropy takes a value close to the von Neumann entropy at high temperature, and its growth rate coincides with the Kolmogorov–Sinaï entropy for the 1D inverted harmonic oscillator [16].

A direct evaluation of the HW entropy for a quantum system is a kind of challenge even for a system with a few degrees of freedom because, apart from the cumbersome calculation with precision of

the logarithm, it involves a large-dimensional integral over the phase space. Nevertheless, the HW entropy and its time evolution have been calculated for some quantum systems [21,22]. The equation of motion (EOM) of the Husimi function is given in Ref. [11], which contains a term of the order $\hbar$, and thus has a more complicated form than that of the Wigner function, even in the semiclassical approximation; see below. To solve the complicated EOM of the Husimi function, a test-particle method was proposed by Tsai and Muller [22], where the evolution of the test particles is determined to reproduce some of the moments.

As already mentioned, the semiclassical approximation is suitable for revealing the effect of the chaotic nature of the classical counterpart. It is noteworthy that the time evolution of the Wigner function in the semiclassical approximation where the $\mathcal{O}\left(\hbar^2\right)$ terms are ignored is readily obtained by solving the classical Hamilton equation; quantum-mechanical information such as the uncertainty relation is encoded in the initial Wigner function, provided that it is given as the Wigner transform of the quantum density matrix.

The time evolution of the Husimi function is given by smearing the time-evolved Wigner function obtained in the semiclassical approximation. This is the method we adopt in this article. We shall show its efficiency and usefulness in describing entropy production using a couple of quantum-mechanical systems whose respective classical counter-systems are known to be chaotic. We propose two methods to evaluate the time evolution of the Husimi–Wehrl entropy. One is an adaptation of the usual test-particle method without recourse to the moments of the distribution function. The other is a sequential application of Monte Carlo integration, which we call the two-step Monte Carlo method. We shall demonstrate the characteristics of the two methods by numerical calculations, and show that simultaneous application of the two methods ensures the reliability of the results of the HW entropy's time evolution. It should be noted that these two methods are, in principle, applicable to systems with large degrees of freedom such as quantum field theories.

The paper is organized as follows. In Sect. 2, we summarize some basic ingredients of the Wigner and Husimi functions together with the HW entropy. In Sect. 3, we introduce the two numerical methods to evaluate the HW entropy in an efficient way. In Sect. 4, the quantum-mechanical models are introduced and numerical results of the Husimi–Wehrl entropy are shown. The final section is devoted to a brief summary and concluding remarks.

2. Wigner function, Husimi function, and Husimi–Wehrl entropy

In this section, we briefly review quantum-mechanical phase space distribution functions, the Wigner [3] and Husimi [9] functions, and the phase space expression of the entropy, Husimi–Wehrl entropy [14]. While we introduce the Wigner and Husimi functions in 1D quantum mechanics in Sects. 2.1 and 2.2, extension to multidimensional cases is straightforward.

2.1. Wigner and Husimi functions
The Wigner function [3] is defined as a Wigner transform of the density matrix

$$f_W\left(q, p, t\right) = \rho_W\left(q, p, t\right)$$
$$\equiv \int d\eta\, e^{-ip\eta/\hbar}\left\langle q + \frac{\eta}{2} \mid \rho\left(t\right) \mid q - \frac{\eta}{2} \right\rangle. \tag{4}$$

While the Wigner function $f_W\left(q, p\right)$ can be regarded as a quasi phase space distribution function and provides an intuitive picture of the phase space dynamics, it is not semi-positive definite; hence, we cannot regard $f_W\left(q, p\right)$ as the phase space probability density.

In order to overcome the above drawbacks of the Wigner function, Husimi introduced a Gaussian-smeared Wigner function [9], known as the Husimi function,

$$f_{\mathrm{H}}(q, p) = \int \frac{dq'dp'}{\pi\hbar} e^{-\Delta(q-q')^2/\hbar - (p-p')^2/\Delta\hbar} f_{\mathrm{W}}(q, p),$$ (5)

where Δ is an arbitrary width parameter that gives the smearing manner in the phase space.

The Husimi function is also defined as the expectation value of the density matrix with respect to a coherent state $|z\rangle$:

$$f_{\mathrm{H}}(q, p) = \langle z|\rho|z\rangle, \quad z = (\Delta q + ip)/\sqrt{2\hbar\Delta},$$ (6)

for a 1D case with Δ being an arbitrary constant. Here the coherent state is given by

$$|z\rangle = e^{za^\dagger - z^* a}|0\rangle, \quad a = (\Delta\hat{q} + i\hat{p})/\sqrt{2\hbar\Delta},$$ (7)

where $|0\rangle$ is the ground state; $\hat{a}|0\rangle = 0$. It is readily shown that $f_{\mathrm{H}}(q, p)$ is *semi-positive definite*, $f_{\mathrm{H}} \geq 0$ by using Eq. (6), $f_{\mathrm{H}} = |\langle z|\psi\rangle|^2 \geq 0$ for a pure state $|\psi\rangle$, and $f_{\mathrm{H}} = \sum_i w_i |\langle z|\psi_i\rangle|^2 \geq 0$ for a mixed state specified by the density matrix $\rho = \sum_i w_i |\psi_i\rangle\langle\psi_i|$ ($w_i \geq 0$).

The Husimi function $f_{\mathrm{H}}(q, p)$ serves as the probability density to observe the phase space variables (q, p) under a minimum wave packet $|z\rangle$, and is now semi-positive definite, $f_{\mathrm{H}} \geq 0$. Compared with the Wigner function, the Husimi function is smooth and the peak of the Husimi function often appears around the expectation value of the position and momentum [11,23].

2.2. Time evolution in the semiclassical approximation

The equation of motion (EOM) for the Wigner function f_{W} is obtained from the Wigner transform of the von Neumann equation for the density matrix, $\partial\rho/\partial t = [H, \rho]/i\hbar$. By applying the Wigner transform of the operator product, $(AB)_{\mathrm{W}} = A_{\mathrm{W}} \exp\left(i\hbar\left(\overleftarrow{\nabla}_q \overrightarrow{\nabla}_p - \overleftarrow{\nabla}_p \overrightarrow{\nabla}_q\right)/2\right) B_{\mathrm{W}}$ [4,5,8], commutators are replaced by Poisson brackets as $[A, B]_{\mathrm{W}}/i\hbar = \{A, B\}_{\mathrm{PB}} + \mathcal{O}\left(\hbar^2\right)$. Thus the EOM for f_{W} is given in terms of the Wigner transform H_{W} of the Hamiltonian H as

$$\frac{\partial f_{\mathrm{W}}}{\partial t} = \{H_{\mathrm{W}}, f_{\mathrm{W}}\}_{\mathrm{PB}} + \mathcal{O}\left(\hbar^2\right).$$ (8)

The Wigner transform H_{W} of a Hamiltonian with the form $H = p^2/2m + U(q)$ does not change its form. We note that the $\mathcal{O}\left(\hbar^2\right)$ term in (8) is proportional to the third derivative of H_{W} or U. Thus the EOM (8) without the $\mathcal{O}\left(\hbar^2\right)$ term turns out to be exact for some simple models such as an (inverted) harmonic oscillator.

The semiclassical EOM for f_{W} is given by retaining the terms up to $\mathcal{O}(\hbar)$ in Eq. (8), which reads

$$\frac{\partial f_{\mathrm{W}}}{\partial t} + \frac{\partial H_{\mathrm{W}}}{\partial p}\frac{\partial f_{\mathrm{W}}}{\partial q} - \frac{\partial H_{\mathrm{W}}}{\partial q}\frac{\partial f_{\mathrm{W}}}{\partial p} = 0.$$ (9)

We remark that the semiclassical EOM is exact for the linear systems mentioned above. Equation (9) asserts that f_{W} is constant along the classical trajectory: Let us see this. Let $(q(t; \bar{q}), p(t; \bar{p}))$ be a solution of the classical EOM, i.e., Hamilton's equation,

$$\frac{dq}{dt} = \frac{\partial H_{\mathrm{W}}}{\partial p}, \quad \frac{dp}{dt} = -\frac{\partial H_{\mathrm{W}}}{\partial q},$$ (10)

with an initial condition $(q(0) = \bar{q}, p(0) = \bar{p})$. Then we have, for $f_{\mathrm{W}}(q(t; \bar{q}), p(t; \bar{p}), t)$,

$$\frac{Df_{\mathrm{W}}}{Dt} \equiv \frac{\partial f_{\mathrm{W}}}{\partial t} + \frac{dq}{dt}\frac{\partial f_{\mathrm{W}}}{\partial q} + \frac{dp}{dt}\frac{\partial f_{\mathrm{W}}}{\partial p} = 0,$$ (11)

which implies that $f_{\rm W}$ is time-independent; $f_{\rm W}\left(q\left(t;\bar{q}\right),\,p\left(t;\bar{p}\right),\,t\right)=f_{\rm W}\left(\bar{q},\,\bar{p},\,0\right)$. Accordingly, we have

$$f_{\rm W}\left(q,\,p,\,t\right)=f_{\rm W}\left(q\left(-t;q\right),\,p\left(-t;p\right),\,0\right). \tag{12}$$

Thus we can obtain the semiclassical time evolution of the Wigner function by solving the classical equation of motion. Note that the quantum-mechanical effects are taken into account through the distribution of the initial value in the phase space encoded in the Wigner function $f_{\rm W}\left(q,\,p,\,0\right)$ constructed from the initial density matrix.

It is worth mentioning that the exact analytical solution of the time evolution of $f_{\rm W}$ for some linear systems including a (stable) harmonic oscillator potential [4,16], an inverted (unstable) harmonic oscillator potential [16,24], and an external potential [16] can be obtained. Then even the analytic form of the Husimi function $f_{\rm H}\left(q,\,p,\,t\right)$ for these systems is readily obtained [16] by the Gaussian smearing of $f_{\rm W}\left(q,\,p,\,t\right)$, which is easy to perform analytically.

We note here that one may obtain the time evolution of the Husimi function $f_{\rm H}\left(q,\,p,\,t\right)$ by solving the EOM for $f_{\rm H}\left(q,\,p,\,t\right)$, which involves terms proportional to $\hbar$ and thus has a more complicated structure than that for $f_{\rm W}\left(q,\,p,\,t\right)$ even in the semiclassical approximation [11]. If one sticks to solving the EOM for $f_{\rm H}$ directly, some numerical method would be necessary. A test-particle method is adopted as such a numerical method by Tsai and Muller [22], where the time evolution of test particles is determined so as to reproduce some of the moments. We remark that there are some ambiguities in such an approach inherent in the moment method.

In this work, we do not adopt this direct method for obtaining the time evolution of the Husimi function $f_{\rm H}\left(q,\,p,\,t\right)$. We take advantage of the fact that the EOM of the Wigner function $f_{\rm W}\left(q,\,p,\,t\right)$ in this regime is given simply by solving the classical EOM, and obtain $f_{\rm H}\left(q,\,p,\,t\right)$ by the Gaussian smearing of the thus-obtained $f_{\rm W}\left(q,\,p,\,t\right)$. This strategy should be workable and natural when the semiclassical approximation is meaningful. The remaining task that we have to do to obtain the Husimi function is just the multidimensional integrations over the phase space with the Gaussian kernel for the smearing, which should be feasible by standard methods such as Monte Carlo integration.

2.3. Husimi–Wehrl entropy

Since the Wigner function $f_{\rm W}$ is merely the Weyl transform of the density matrix, any observable is calculable in terms of $f_{\rm W}$ in principle, and this is also the case with the Husimi function $f_{\rm H}$. A drawback of the $f_{\rm W}$ is that it can have negative values; hence, it is not suitable for the calculation of entropy. As mentioned in the introduction and the previous subsection, the Husimi function is, in contrast, a semi-positive definite *coarse-grained* phase space distribution function smeared by a minimum wave packet; hence, it is a good candidate for the phase space distribution $f\left(q,\,p\right)$ to evaluate the entropy of a quantum system, as Boltzmann's H function in the classical system, Eq. (2), or, equivalently, the Husimi–Wehrl entropy given in Eq. (3) [14].

An explicit form of the HW entropy in terms of the Wigner function is given by substituting the D-dimensional extension of Eq. (5) into Eq. (3):

$$S_{\rm HW}\left(t\right)=-\int\frac{d^{D}q\,d^{D}p}{\left(2\pi\hbar\right)^{D}}\int\frac{d^{D}q'\,d^{D}p'}{\left(\pi\hbar\right)^{D}}e^{-\Delta\left(q-q'\right)^{2}/\hbar-\left(p-p'\right)^{2}/\Delta\hbar}f_{\rm W}\left(q',p',t\right)$$

$$\times\log\left[\int\frac{d^{D}q''\,d^{D}p''}{\left(\pi\hbar\right)^{D}}e^{-\Delta\left(q-q''\right)^{2}/\hbar-\left(p-p''\right)^{2}/\Delta\hbar}f_{\rm W}\left(q'',p'',t\right)\right]. \tag{13}$$

One may now recognize some difficulty of the numerical evaluation of the HW entropy: It involves repeated numerical integrations over the multidimensional phase space, and one of them in particular appears as an argument of the logarithm, which turns out to be quite problematic in the Monte Carlo integration.

3. Numerical methods to analyze the semiclassical time evolution of Husimi–Wehrl entropy

Here, two numerical methods are introduced to calculate the time dependence of the HW entropy as given by the Gaussian smearing of the Wigner function obtained in the semiclassical approximation. Both methods are based on an adaptation of the Monte Carlo integration over the phase space. We call the two methods the test-particle (TP) and two-step Monte Carlo (tsMC) methods, respectively. In this section, we deal with the D-dimensional system described by the Hamiltonian $H = H(q, p)$, where q and p denote the D-dimensional vector, respectively, i.e., $q = (q_1, q_2, \ldots, q_D)$ and $p = (p_1, p_2, \ldots, p_D)$.

3.1. Test-particle method
In the test-particle method [25–28], the Wigner function is represented as a sum of the delta functions

$$f_W(q, p, t) = \frac{(2\pi\hbar)^D}{N_{TP}} \sum_{i=1}^{N_{TP}} \delta^D(q - q_i(t)) \, \delta^D(p - p_i(t)), \qquad (14)$$

with the initial function

$$f_W(q, p, 0) = \frac{(2\pi\hbar)^D}{N_{TP}} \sum_{i=1}^{N_{TP}} \delta^D(q - q_i(0)) \, \delta^D(p - p_i(0)),$$

where N_{TP} is the total number of test particles, and their coordinates are given by $(q_i(t), p_i(t))$. The initial distribution of the test particles $(q_i(0), p_i(0))$ $(i = 1, 2, \ldots, D)$ is chosen so as to well sample that of $f_W(q, p, 0)$; hence, N_{TP} is called the sampling number. The time evolution of the coordinates $(q_i(t), p_i(t))$ is determined by the EOM for $f_W(q, p, t)$, which is reduced to the canonical equation of motion,

$$\frac{dq_i}{dt} = \frac{\partial H_W}{\partial p_i}, \quad \frac{dp_i}{dt} = -\frac{\partial H_W}{\partial q_i}, \qquad (15)$$

in the semiclassical approximation.

For the test-particle representation of the Wigner function, Eq. (14), the Husimi function is readily expressed as

$$f_H(q, p, t) = \frac{2^D}{N_{TP}} \sum_{i=1}^{N_{TP}} e^{-\Delta(q - q_i(t))^2/\hbar - (p - p_i(t))^2/\Delta\hbar}. \qquad (16)$$

It is noteworthy that the Husimi function here is a smooth function in contrast to the corresponding Wigner function in Eq. (14).

Inserting the Wigner function (14) into Eq. (13), the HW entropy in the test-particle method is given as

$$S_{HW}^{(TP)} = -\frac{1}{N_{TP}} \sum_{i=1}^{N_{TP}} \int \frac{d^D q \, d^D p}{(\pi\hbar)^D} e^{-\Delta(q - q_i(t))^2/\hbar - (p - p_i(t))^2/\Delta\hbar} \log f_H(q, p, t). \qquad (17)$$

Now note that the integral over $(q, p)_i$ for each i has a support only around the positions of the test particles $(q_i(t), p_i(t))$ due to the Gaussian function, and then we can effectively perform the

Monte Carlo integration as follows. By generating a set of random numbers $(Q, P)_i$ with standard deviations of $\sqrt{\hbar/2\Delta}$ and $\sqrt{\hbar\Delta/2}$, the Monte Carlo sampling point $(q, p)_i$ for each i is obtained as $(q, p)_i = (Q, P)_i + (q_i, p_i)$. Thus we reach the formula to be used in the actual evaluation of the HW entropy in the test-particle method:

$$S_{\mathrm{HW}}^{(\mathrm{TP})} \simeq -\frac{1}{N_{\mathrm{MC}}N_{\mathrm{TP}}} \sum_{k=1}^{N_{\mathrm{MC}}} \sum_{i=1}^{N_{\mathrm{TP}}} \log \left[\frac{2^D}{N_{\mathrm{TP}}} \sum_{j=1}^{N_{\mathrm{TP}}} e^{-\Delta\left(Q_k+q_i(t)-q_j(t)\right)^2/\hbar - \left(P_k+p_i(t)-p_j(t)\right)^2/\Delta\hbar} \right], \quad (18)$$

where N_{MC} denotes the sample number of $(Q, P)_i$.

3.2. Two-step Monte Carlo method

The second method is a direct Monte Carlo evaluation of the multidimensional integrals. We rewrite Eq. (13) as

$$S_{\mathrm{HW}}^{(\mathrm{tsMC})} = -\int \frac{d^D Q d^D P}{(\pi\hbar)^D} e^{-\Delta Q^2/\hbar - P^2/\Delta\hbar} \int \frac{d^D q d^D p}{(2\pi\hbar)^D} f_{\mathrm{W}}(q, p, t)$$

$$\times \log \left[\int \frac{d^D Q' d^D P'}{(\pi\hbar)^D} e^{-\Delta(Q')^2/\hbar - (P')^2/\Delta\hbar} f_{\mathrm{W}}\left(q + Q + Q', p + P + P', t\right) \right]$$

$$\simeq -\frac{1}{N_{\mathrm{out}}} \sum_{k=1}^{N_{\mathrm{out}}} \log \left[\frac{1}{N_{\mathrm{in}}} \sum_{l=1}^{N_{\mathrm{in}}} f_{\mathrm{W}}\left(q_k + Q_k + Q_l', p_k + P_k + P_l', t\right) \right]$$

$$= -\left\langle \log \left\langle f_{\mathrm{W}}\left(q + Q + Q', p + P + P', t\right)\right\rangle_{Q'P'} \right\rangle_{QPqp}, \quad (19)$$

where (Q_k, P_k) and $\left(Q_l', P_l'\right)$ are Gaussian random numbers for the Monte Carlo (MC) integration to compute the Husimi function $f_{\mathrm{H}}(q, p)$. For the (q, p) integration, we generate MC samples (q', p') at $t = 0$ according to the initial distribution, and obtain the corresponding phase space sample points $(q(q', p', t), p(q', p', t))$ at t by solving the canonical equation of motion. Under the semiclassical approximation, f_{W} is constant and the Jacobian is unity along the classical trajectory, $J(q(t), p(t)/q'(0), p'(0)) = 1$. Then we can replace the integral over (q, p) in the first line of Eq. (19) with the integral at $t = 0$ by using the initial distribution and the Liouville theorem as

$$\int \frac{d^D q d^D p}{(2\pi\hbar)^D} f_{\mathrm{W}}(q, p, t) g(q, p) = \int \frac{d^D q' d^D p'}{(2\pi\hbar)^D} f_{\mathrm{W}}(q', p', 0) g(q(q', p', t), p(q', p', t)), \quad (20)$$

where (q', p') are the phase space coordinates at $t = 0$, and $(q(q', p', t), p(q', p', t))$ are those at t evolved from (q', p').

The Wigner function at t in the log in Eq. (19) can be obtained by the trace back of the trajectory from t to $t = 0$, as shown in Eq. (12). Equation (19) contains an MC integral of a function obtained by an MC integral; we first generate (q', p') at $t = 0$ according to the distribution $f_{\mathrm{W}}(q, p, 0)$ and (Q, P) as Gaussian random numbers, and then perform the MC integral in the log by generating MC samples (Q', P'). We call this procedure *two-step Monte Carlo* (tsMC).

In the following sections, we show the characteristic properties of the two methods and demonstrate numerically how they work using 2D quantum-mechanical systems.

4. Numerical calculation of Husimi–Wehrl entropy in the quantum Yang–Mills model

In this section, we show the numerical results of the HW entropy in a "quantum Yang–Mills system" [29], obtained by the two distinct methods, TP and tsMC.

4.1. Model Hamiltonian and setup of initial condition

The Hamiltonian of the system is given by

$$H = \frac{1}{2m}\left(p_1^2 + p_2^2\right) + \frac{1}{2}q_1^2 q_2^2. \tag{21}$$

We have restricted ourselves to the 2D case here. The name "quantum Yang–Mills (qYM)" originates from the fact that the spatially uniform Yang–Mills system is reduced to a $(0 + 1)$-dimensional system, i.e., a quantum-mechanical system, and its Hamiltonian is just given by Eq. (21).

We adopt the initial condition given by a minimal wave packet centered at $(q_1, q_2, p_1, p_2) = (0, 0, 10, 10)$:

$$f_W\left(p_1, p_2, q_1, q_2, t = 0\right) = 4e^{-[q_1^2 + q_2^2 + (p_1 - 10)^2 + (p_2 - 10)^2]/\hbar}. \tag{22}$$

This initial condition is also adopted in Ref. [22].

In the following, we show numerical results calculated by using the TP and tsMC methods. We show the results in units with $m = 1$ and $\hbar = 1$, and take $\Delta = 1$ for the wave-packet width. In the case of $\Delta \neq 1$, the smearing Gaussian is not symmetric in the p and q directions. However, the results do not change qualitatively. We have confirmed that the results with $\Delta = 0.1$ and 10 are qualitatively the same as those with $\Delta = 1$.

4.2. Numerical results with the TP method

First, we show the numerical results of the HW entropy in the qYM system calculated in the TP method using Eq. (18).

Figure 1 shows the time evolution of the HW entropy calculated in the TP method with the following test-particle numbers: $N_{TP} = 100, 1000, 5000,$ and $15\,000$. The MC sample number is taken to be $N_{MC} = 500$. The statistical errors are estimated for N_{MC} samples from a standard deviation. We note that the calculated HW entropy at each t tends to increase along with increasing N_{TP}, which is
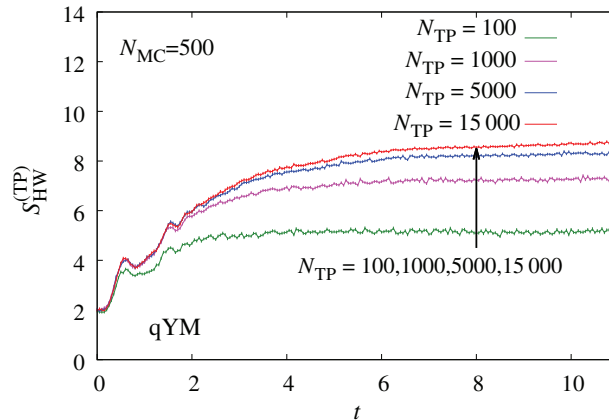

Fig. 1. Time dependence of the HW entropy by using the TP method in qYM, with $N_{TP} = 100, 1000, 5000,$ and $15\,000$, and $N_{MC} = 500$. The arrow shows how the calculated HW entropy changes as N_{TP} increases.

an artifact due to the small number of the test particles N_{TP} and will be discussed later. Apart from tiny fluctuations, all the calculations show that the HW entropy first increases with time, accompanied by a small oscillatory behavior; its local maxima are seen around $t \simeq 0.5$ and 1.7. We note that a similar behavior is also seen in Ref. [22].

Entropy evaluated by the TP method has an (unphysical) maximum depending on N_{TP}, which causes apparent saturation at large t in Fig. 1. In fact, when the system is chaotic and the phase space volume is very large, all the test particles will be so separated from each other in the phase space at later time that only the $i = j$ terms in Eq. (18) will remain. In this limiting case, the HW entropy as given in (18) is evaluated as follows:

$$S_{HW}^{(TP)} \rightarrow - \left\langle \left[\log \left(\frac{2^D}{N_{TP}} \right) - \Delta Q^2/\hbar - P^2/\Delta \hbar \right] \right\rangle_{QP}$$
$$= D - D \log 2 + \log N_{TP}, \tag{23}$$

which gives the inevitable upper limit of $S_{HW}^{(TP)}$. In Appendix A, we examine the HW entropy of an inverted harmonic oscillator, for which S_{HW} can be calculated analytically and is found to increase permanently. At later times, S_{HW} is underestimated with small N_{TP} values because of the upper limit discussed above. By comparison, S_{HW} at early times is calculated precisely in the TP method, as long as N_{TP} is large enough for S_{HW} to converge.

From the above argument, $S_{HW}(t)$ would be obtained reliably as an extrapolated value in the limit of $N_{TP} \rightarrow \infty$. The extrapolation should be made in the N_{TP} range, where the limiting value is larger than the HW entropy to be obtained. The limiting values are $S_{HW}^{(TP)} = 5.2, 7.5, 9.1$, and 10.2 for $N_{TP} = 100, 1000, 5000$, and $15\,000$, respectively. The large-t values found in Fig. 1 are close to these limiting values for smaller N_{TP}, i.e., $N_{TP} = 100$ and 1000. Thus we see that the saturation behavior seen for smaller values of N_{TP} may be an artifact of the TP method. In contrast, the large-t values for $N_{TP} = 5000$ and $15\,000$ in Fig. 1 are well below the limiting values (9.1 and 10.2), found free from the above-mentioned artifact, and can be used to obtain the extrapolated value at $N_{TP} \rightarrow \infty$, as discussed later in Sect. 4.4. Thus we conclude that the entropy production of the "quantum Yang–Mills" system can be well described with the use of HW entropy as calculated with the TP method with a sufficiently large number of test particles.

4.3. Numerical results with the tsMC method

Next, we show the numerical results of the HW entropy in qYM in the tsMC method using the formula Eq. (19).

Figure 2 shows the time evolution of the HW entropy calculated in the tsMC method with the sample numbers $N_{in} = 1200, 2400, 4800$, and $12\,000$. N_{out} is taken to be the same as N_{in}. The errors attached to S_{HW} in the present figure are estimated only for the Monte Carlo integrals outside the log in Eq. (19), and those from the integral inside the log are not taken into account, which causes an additional systematic error.

We see that the larger the value of N_{in}, the smaller the HW entropy, which is an opposite dependence on the sample number to that in the TP method. Nevertheless, the gross behavior in the time evolution of the HW entropy is quite similar in the two methods apart from tiny fluctuations: After showing an oscillatory behavior in the first short period, it increases in a monotonous way and its growth rate decreases gradually. A more quantitative comparison of the two methods will be presented in the next subsection.
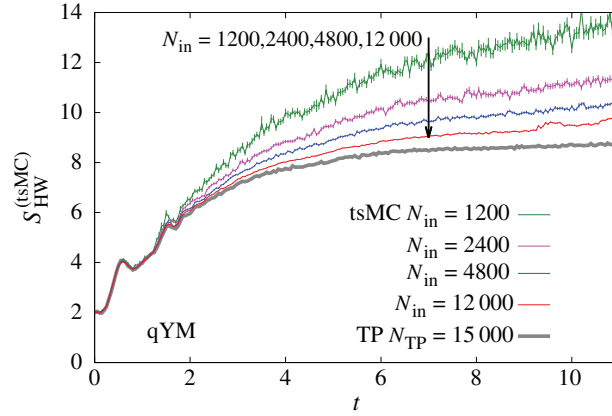
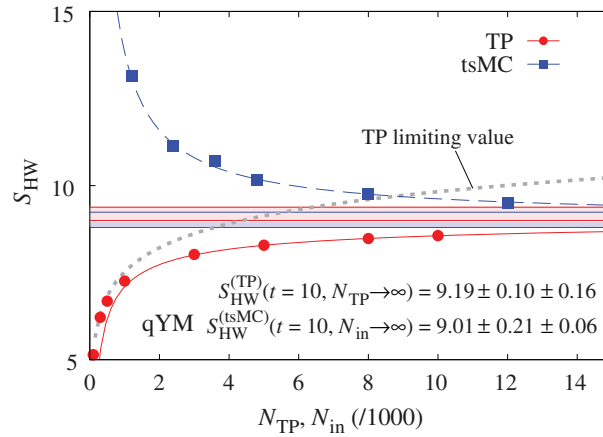**Fig. 2.** Time dependence of HW entropy calculated by using the tsMC method.

Fig. 3. HW entropy in qYM at $t = 10$ as a function of N_{TP} (N_{MC}), and its extrapolation to infinitely large N_{TP} (N_{MC}) in the TP (tsMC) method. Filled circles (squares) show the TP (tsMC) results, and the solid (dashed) line shows a fit function to the TP (tsMC) results. The dotted line is a limiting value given by Eq. (23). The shaded areas show the extrapolated value in the limit of $N_{\mathrm{TP}}, N_{\mathrm{MC}} \to \infty$.

4.4. Comparison of the two methods

Figure 3 shows the HW entropy at $t = 10$ as a function of N_{TP} (N_{in}) in the TP (tsMC) method. We fit a linear function $f(t) = at + b$ to the calculated $S_{\mathrm{HW}}(t)$ data in the range $10 - \Delta t \le t \le 10 + \Delta t$ ($\Delta t = 1$), and adopt $f(t = 10)$ as the HW entropy value at $t = 10$. This procedure provides a smoother curve and reduces the errors coming from fluctuations compared to directly using the raw data.

The HW entropy in the TP method becomes larger with increasing N_{TP}, as already mentioned: At $t = 10$, $S_{\mathrm{HW}} \simeq 5.1$ for $N_{\mathrm{TP}} = 100$ and $S_{\mathrm{HW}} \simeq 8.7$ for $N_{\mathrm{TP}} = 15\,000$. We also show the fit results to the data for larger samples, say $N_{\mathrm{TP}} \ge 5000$, with a fit function

$$f(N) = a - \frac{b}{N^c}. \tag{24}$$

The extrapolated value to $N_{\mathrm{TP}} \to \infty$ is 9.19 ± 0.10. When we use other fit functions such as $f(N) = a - b/(N/c + 1)$ and $f(N) = a - b/N + c/N^2$, the fit results have differences with a standard deviation of 0.16, which should be considered as a systematic error. Thus the HW entropy in the

TP method is obtained as

$$S_{\mathrm{HW}}^{(\mathrm{TP})}\,(t=10)=9.19\pm0.10\,\text{(stat.)}\pm0.16\,\text{(syst.)}. \qquad (25)$$

With increasing N_{in}, the HW entropy calculated in the tsMC method decreases, which is an opposite behavior to that in the TP method, as noted before. At $t=10$, $S_{\mathrm{HW}}\simeq13.2$ for $N_{\mathrm{in}}=1200$ and $S_{\mathrm{HW}}\simeq9.5$ for $N_{\mathrm{in}}=12\,000$. We also show the fit results to the data. We adopt Eq. (24) for the fit function. From the fit results, the HW entropy in the tsMC method is found to be

$$S_{\mathrm{HW}}^{(\mathrm{tsMC})}\,(t=10)=9.01\pm0.21\,\text{(stat.)}\pm0.06\,\text{(syst.)}, \qquad (26)$$

where the central value and the statistical error are obtained from the fit using Eq. (24), and the systematic error is evaluated from the fits using several fit functions, as done in the TP method.

4.5. Discussions

The time evolutions of the HW entropies obtained in the TP and tsMC methods both show similar behavior: The HW entropy increases with an oscillatory behavior in the early stage, then shows a monotonous increase with a decreasing rate. The HW entropy at each t in the TP method increases along with N_{TP}, while it decreases with increasing N_{in} in the tsMC method. Thus we can guess that the real value of the HW entropy lies between the results in the TP and tsMC methods. Actually, the extrapolated values at $t=10$, $S_{\mathrm{HW}}^{(\mathrm{TP})}\,(t=10)=9.19\pm0.10\pm0.16$ at $N_{\mathrm{TP}}\to\infty$ and $S_{\mathrm{HW}}^{(\mathrm{tsMC})}\,(t=10)=9.01\pm0.21\pm0.06$ at $N_{\mathrm{in}}\to\infty$ in the TP and tsMC methods, respectively, are consistent with each other within the error. These results are also in agreement with that in Ref. [22].

These two methods, TP and tsMC, give consistent results after $N\to\infty$ extrapolation. On the other hand, with finite N_{TP} and N_{in}, they could give seemingly inconsistent results depending on the dynamics. We here have a deeper look at this issue. In the tsMC method, the entropy seems to keep increasing even for later times, in contrast to the results in the TP method with finite N_{TP} and in Ref. [22]. The discrepancy may come from the special shape of the potential: there are two flat directions in the potential for the qYM system, although the width of them tends to shrink at large distances. Then, the classical trajectory can keep growing along the flat direction, which would cause an unlimited spreading of the Husimi function and a permanent increase of the HW entropy calculated in the semiclassical approximation. (In the case of the TP methods, there exists a limiting value of the HW entropy depending on N_{TP}, which gives rise to the apparent saturation of S at large t.) By comparison, it is shown that the exact energy spectra of the qYM are all discrete ones, because of the shrinking width leading to an increase of the kinetic energy due to the uncertainty relation, although the volume of $\{(p,q)\,|\,H\,(p,q)\le E\}$ is infinite [30]. Note that the discrete spectra imply that the wave functions of the energy eigenstates are all bound. Thus the corresponding Husimi function would not have support at an infinite distance due to the quantum effect, and the HW entropy may not show ever-increasing behavior but have a saturated value. This plausible conjecture can only be confirmed by a full quantum calculation beyond the semiclassical approximation. Such a calculation is beyond the scope of the present work and will be left for future work. Instead, we shall take another model, which is a modified version of the qYM one free from flat directions in its potential.

5. Modified quantum Yang–Mills model

Let us consider the model in which quartic potential terms are added to the qYM Hamiltonian:

$$H=\frac{p_1^2}{2m}+\frac{p_1^2}{2m}+\frac{1}{2}g^2q_1^2q_2^2+\frac{\epsilon}{4}q_1^4+\frac{\epsilon}{4}q_2^4. \qquad (27)$$
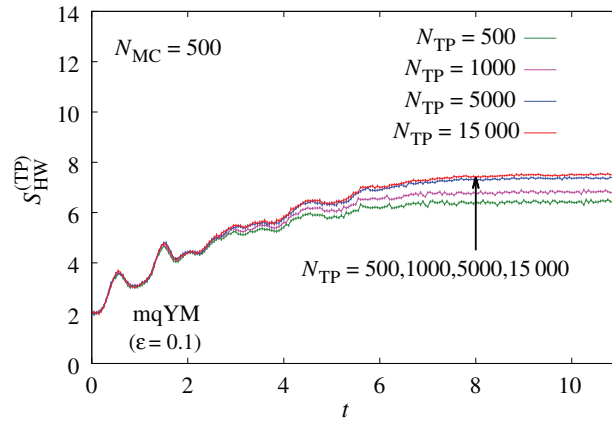
Fig. 4. Time dependence of HW entropy by using the TP method in modified qYM.
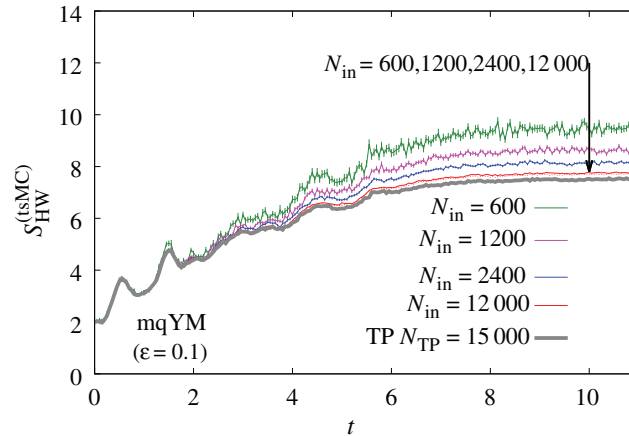

Fig. 5. Time dependence of HW entropy by using the tsMC method in modified qYM.

We call the system "modified quantum Yang–Mills (mqYM)". The system is studied in Refs. [12,13] with $g^2 < 0$ in the context of chaos. It is apparent that there is no flat direction in the potential due to the quartic terms. We take $g^2 = 1$ and $\epsilon = 0.1$ in the Hamiltonian, Eq. (27). The mqYM system is found to be integrable with $\epsilon/g^2 = 1, 1/3$, and ∞ [13,31]. Our choice of $\epsilon/g^2 = 0.1$ is well apart from the integrable region. Since ϵ is not very large, the HW entropy shows a similar behavior to that in qYM at early times, as shown later.

   In this section, we shall calculate the HW entropy of the mqYM system in the TP and tsMC methods. The analyses are carried out in a similar way to those for the qYM system.

   In Figs. 4 and 5, we show the time evolution of the HW entropy in mqYM calculated using the TP ($N_{\mathrm{TP}} = 500, 1000, 5000$, and $15\,000$ with $N_{\mathrm{MC}} = 500$) and tsMC ($N_{\mathrm{in}} = 600, 1200, 2400$, and $12\,000$) methods, respectively. N_{out} is taken to be the same as N_{in} for tsMC.

   The distribution function in Eq. (22) is used as the initial condition, and the statistical errors are estimated for N_{MC} (N_{in}) samples from a standard deviation in the TP (tsMC) method, as in the qYM cases.

   Both of the calculated results show that the HW entropy first increases with an oscillatory behavior and tends to saturate at later times, $t \gtrsim 6$. The later-time S_{HW} values depend on the sample number, N_{TP} and N_{in}: With increasing N_{TP} (N_{in}), the HW entropy increases (decreases) in the TP (tsMC)
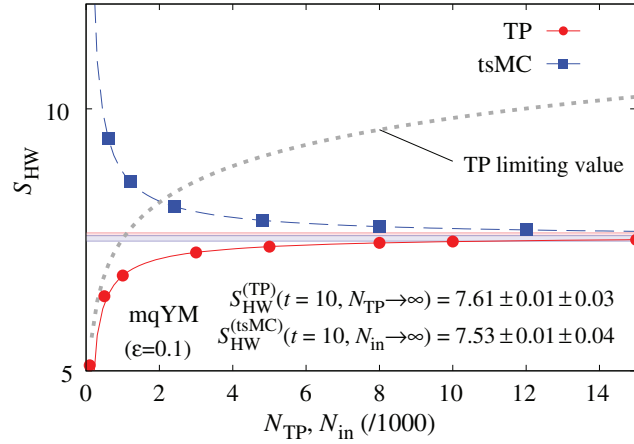
Fig. 6. HW entropy in mqYM at $t = 10$ as a function of N_{TP} (N_{MC}), and its extrapolation to infinitely large N_{TP} (N_{MC}) in the TP (tsMC) method. Filled circles (squares) show the TP (tsMC) results, and the solid (dashed) line shows a fit function to the TP (tsMC) results. The dotted line is a limiting value given by Eq. (23). The shaded areas show the extrapolated value in the limit of N_{TP}, $N_{MC} \to \infty$.

method. These are the features also found in qYM. By comparison, it should be noted that there seems to be saturation of S_{HW} in both the TP and tsMC methods in mqYM, in contrast to qYM. This may originate from the finite phase space volume where the Husimi function has support.

In Fig. 6, we show the HW entropy at $t = 10$ as a function of N_{TP} or N_{in}. We fit a linear function to the calculated $S_{HW}(t)$ results in the range $9 < t < 11$, and adopt $f(t = 10)$ as the HW entropy value at $t = 10$. In the TP method, $S_{HW}^{(TP)}(t = 10) \simeq 6.4$ and 7.5 for $N_{TP} = 500$ and $15\,000$, respectively. In tsMC, we find $S_{HW}^{(tsMC)}(t = 10) \simeq 9.4$ and 7.7 for $N_{in} = 600$ and $12\,000$, respectively.

The extrapolated values of S_{HW} at $N_{TP} \to \infty$ and $N_{in} \to \infty$ are found to be

$$S_{HW}^{(TP)}(t = 10) = 7.61 \pm 0.01 \,(\text{stat.}) \pm 0.03 \,(\text{syst.}), \tag{28}$$

$$S_{HW}^{(tsMC)}(t = 10) = 7.53 \pm 0.01 \,(\text{stat.}) \pm 0.04 \,(\text{syst.}), \tag{29}$$

in the TP and tsMC methods, respectively. The central values and the statistical errors are obtained from the fit using Eq. (24), and the systematic error is evaluated from the fits using several fit functions. These two values are consistent with each other within the error.

The observation shows that the two methods, tsMC and TP, are especially effective for such a potential that bounds the Husimi function in a finite region. Thus, we are confident of the validity of the two methods in the mqYM system.

6.   Summary

We have discussed entropy creation in isolated quantum systems by using the Husimi–Wehrl entropy evaluated in a semiclassical treatment. The semiclassical treatment is known to be useful in some systems, such as inflation in the early universe and the early stage of relativistic heavy-ion collisions. These systems are expected to bear instabilities and/or chaoticities in their classical counter-systems; then the smearing of the phase space distribution by the minimal wave packet causes entropy production in terms of the Wehrl entropy or Boltzmann's H function even in isolated quantum systems. This is nothing but the Husimi–Wehrl entropy, the Wehrl entropy obtained by using the Gaussian-smeared Wigner function (Husimi function) for the phase space distribution.

The semiclassical time evolution of the Husimi function is given by solving a classical equation of motion and smearing with a Gaussian packet. Combining this semiclassical treatment with the Monte Carlo numerical integral technique, we have developed two methods, the test-particle (TP) method and the two-step Monte Carlo (tsMC) method. We have applied these two methods to quantum-mechanical systems in two dimensions, the quantum Yang–Mills (qYM) and the modified quantum Yang–Mills (mqYM) systems. The classical counter-systems of these are known to be chaotic. We have demonstrated that the Husimi–Wehrl entropy obtained in the TP (tsMC) method approaches the converged value from below (from above) with an increasing sample number; we can then guess the true value of HW entropy. We have further found that the results of the TP and tsMC methods in the infinite sampling number limit are consistent within the error. Therefore, simultaneous application of the two methods ensures the reliability of the results of the Husimi–Wehrl entropy at a given time.

The extension of our methods to a multidimensional system is straightforward. We expect that these methods will be useful in systems with many degrees of freedom, such as quantum field theory. These methods are, in principle, applicable to higher-dimensional problems, and we have confirmed that they actually work in 3D and 4D systems. In higher dimensions, we need many more Monte Carlo samples to obtain statistically reliable results, and it would be necessary to make some approximations for practical purposes. Work in this direction is in progress.

Appendix A.   HW entropy in inverted harmonics

The inverted harmonic oscillator (IHO) is an unstable system, where the Hamiltonian is given as

$$H = \frac{p^2}{2m} - \frac{1}{2}\lambda^2 q^2. \tag{A1}$$

In this system, the classical trajectories are not restricted to a finite region, but extend to infinitely large spatial and momentum regions. While this unbounded nature makes the numerical calculation difficult, the analytic expression of the HW entropy is known [16]. Then, by comparing the numerical results with the analytic solution, we can examine the validity and the precision of the numerical methods.

A.1.   Analytic solution

When the initial distribution of the Wigner function is given by a Gaussian,

$$f_{\mathrm{W}}(p, q; t = 0) = 2 \exp\left(-\frac{1}{\hbar\omega}p^2 - \frac{\omega}{\hbar}q^2\right), \tag{A2}$$

the time evolution of the HW entropy is obtained analytically [16]. Since the potential is quadratic, the semiclassical analysis is exact, and the time evolution of the Wigner function is calculated by
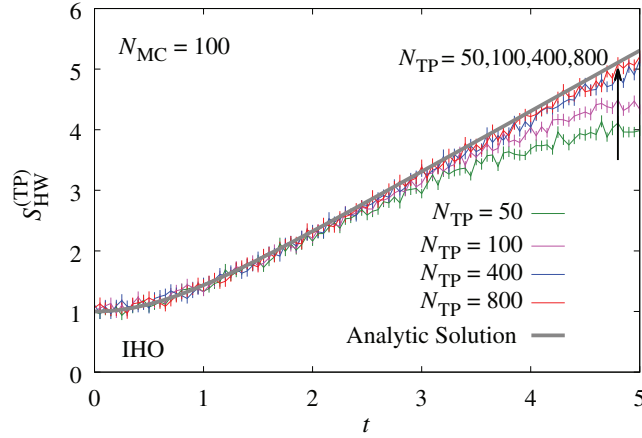
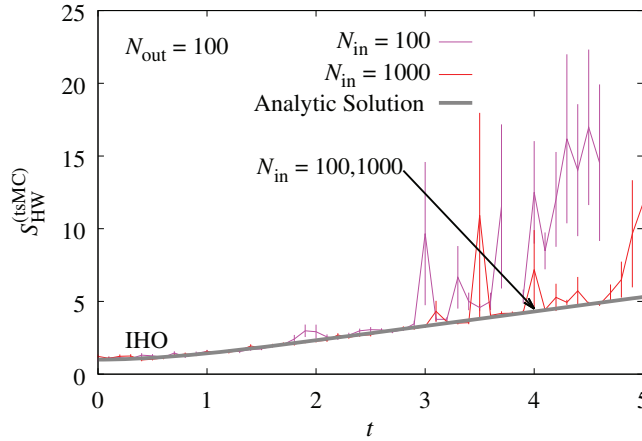**Fig. A1.** Time dependence of the HW entropy of the inverted harmonic oscillator in the TP method.

Fig. A2. Time dependence of the HW entropy of the inverted harmonic oscillator in the tsMC method.

solving the classical equation of motion. The HW entropy at time t is given as [16]

$$S_{\text{HW}}(t) = \log \frac{\sqrt{A(t)}}{2} + 1, \tag{A3}$$

$$A(t) = 2\left(\sigma\rho\cosh(2\lambda t) + 1 + \delta\delta'\right), \tag{A4}$$

$$\sigma = \frac{\lambda^2 + \omega^2}{2\lambda\omega}, \quad \delta = \frac{\lambda^2 - \omega^2}{2\lambda\omega}, \tag{A5}$$

$$\rho = \frac{\Delta^2 + \lambda^2}{2\Delta\lambda}, \quad \delta' = \frac{\Delta^2 - \lambda^2}{2\Delta\lambda}. \tag{A6}$$

A.2.   Numerical results with TP

Figure A1 shows the time evolution of the HW entropy of IHO calculated in the TP method with $N_{\text{TP}} = 50$–800. We find that the TP method can well describe the time evolution of the HW entropy at early times, and that numerical results show saturated behavior at later times. Since there exists a limiting value of S_{HW} in the TP method, as discussed in Sect. 4.2, we need to take a large number of N_{TP} to describe a large amount of entropy production. It should be noted that numerical results converge in the limit of $N_{\text{TP}} \to \infty$, and the converged result well describes the analytic result.

A.3.   Numerical results with tsMC in inverted harmonics

Figure A2 shows the time evolution of the HW entropy of IHO in the tsMC method with $N_{\mathrm{in}} = N_{\mathrm{out}} = 100$ and 1000. We find that the numerical results are consistent with the analytic solution at early times $t \leq 3$, but that the numerical results tend to overestimate the analytic results and numerical errors become very large at later times. A large error would come from the poor overlap between the Wigner function and the coarse-graining Gaussian function at later time, which spoils the importance sampling. On the other hand, the systematic overestimation may be due to the lack of sampling points in the Monte Carlo integration in the logarithmic function (see Eq. (19)). We note here that the statistical-error estimation is performed only for the Monte Carlo integration outside the log.

References

[1] J. von Neumann, Nachr. Ges. Wiss. Göttingen, Math. Phys. Kl. **1927**, 273 (1927).
[2] J. von Neumann, *Mathematische Grundlagen der Quantenmechanik* (Springer, Berlin, 1932).
[3] E. P. Wigner, Phys. Rev. **40**, 749 (1932).
[4] H. Groenewold, Physica **12**, 405 (1946).
[5] J. E. Moyal, Proc. Cambridge Phil. Soc. **45**, 99 (1949).
[6] M. Hillery, R. F. O'Connell, M. O. Scully, and E. P. Wigner, Phys. Rep. **106**, 121 (1984).
[7] H.-W. Lee, Phys. Rep. **259**, 147 (1995).
[8] T. L. Curtright, D. B. Fairlie, and C. K. Zachos, *A Concise Treatise on Quantum Mechanics in Phase Space* (World Scientific, Singapore, 2014).
[9] K. Husimi, Proc. Phys. Math. Soc. Jpn. **22**, 264 (1940).
[10] K. Takahashi and N. Saito, Phys. Rev. Lett. **56**, 645 (1985).
[11] K. Takahashi, Prog. Theor. Phys. Suppl. **98**, 109 (1989).
[12] A. Sugita, J. Phys. A **34**, 9081 (2003).
[13] A. Sugita and H. Aiba, Phys. Rev. E **65**, 036205 (2002).
[14] A. Wehrl, Rev. Mod. Phys. **50**, 221 (1978).
[15] A. Anderson and J. J. Halliwell, Phys. Rev. D **48**, 2753 (1993).
[16] T. Kunihiro, B. Muller, A. Ohnishi, and A. Schafer, Prog. Theor. Phys. **121**, 555 (2009).
[17] F. Mintert and K. Zyczkowski, Phys. Rev. A **69**, 022317 (2004).
[18] M. Abdel-Aty, Prog. Quantum Electron. **31**, 1 (2007).
[19] A. Wehrl, Rep. Math. Phys. **16**, 353 (1979).
[20] E. H. Lieb, Commun. Math. Phys. **62**, 35 (1978).
[21] A. Orlowski, H. Paul, and G. Kastelewicz, Phys. Rev. A **52**, 1621 (1995).
[22] H. M. Tsai and B. Muller, Phys. Rev. E **85**, 011110 (2012).
[23] K. Takahashi, J. Phys. Soc. Jpn. **55**, 762 (1986).
[24] W. H. Zurek and J. P. Paz, Phys. Rev. Lett. **72**, 2508 (1994).
[25] C. Y. Wong, Phys. Rev. C **25**, 1460 (1982).
[26] G. F. Bertsch and S. Das Gupta, Phys. Rep. **160**, 189 (1988).
[27] N. Rostoker and M. N. Rosenbluth, Phys. Fluids **3**, 1 (1960).
[28] R. W. Hockney and J. W. Eastwood, *Computer Simulation using Particles* (CRC Press, London, 1988).
[29] S. G. Matinyan, G. K. Savvidy, and N. G. Ter-Arutyunyan-Savvidy, Zh. Eksp. Teor. Fiz. **80**, 830 (1981). [Sov. Phys. J. Exp. Theor. Phys. **53**, 421 (1981)].
[30] B. Simon, Ann. Phys. **146**, 209 (1983).
[31] S. Baker, V. Z. Enolsky, and A. P. Fordy, Phys. Lett. A **201**, 167 (1995).